Nanomed Res J 6(2):158-169, Spring 2021

RESEARCH ARTICLE

A new ethosomal nanoparticle for controlled release of black cumin compounds against cancer cells

Shilan Nasri[1], Mahdi Rahaie[1,*], Bahman Ebrahimi-Hosseinzadeh[1,*], Ashrafalsadat Hatamian-Zarmi[1], Razi Sahraeian[2]

[1] Department of Life Science Engineering, Faculty of New Sciences and Technologies, University of Tehran, Tehran, Iran

[2] Iran Polymer and Petrochemical Institute, Tehran, Iran

ARTICLE INFO

Article History:
Received 01 Mar 2021
Accepted 28 Apr 2021
Published 01 May 2021

Keywords:
Ethosome
Black cumin
Nanocarrier
Breast cancer
Cytotoxicity

ABSTRACT

Black cumin contains biologically active compounds such as Thymoquinone, which have strong anti-cancer properties. However, most of these agents have poor stability and solubility that limits their use as drugs. In this work, an anti-cancer ethosomal nanostructure containing black cumin extract (BCE) was prepared to release as transdermal-controlled. After synthesis and evaluation of the vesicles for size and charge, as well as determining the ratio of in vitro and ex vivo permeability, experiments to assay their cell toxicity and apoptosis were also investigated. It was confirmed the stable shape (containing 5% soy lecithin, 45% ethanol, and 1.5% cholesterol with a ζ-potential of -61±2 and PDI of 0.14± 0.01.), spherical morphology (20nm) and the effective release rate (40% after 24h in ex vivo permeability test) of these loaded ethosomal nanocarriers using the HPLC, DLS, FTIR, TGA methods and the in vitro and ex vivo release tests. MTT bioassay with BCE (96µg/ml compared to 200 µg/ml) and DOX separately and their ethosomal forms showed the higher cellular toxicity of ethosomic forms on MCF-7. Flow cytometry also proved strong apoptosis in the MCF-7 cells treated with ethosomal compared to non-ethosomal forms (~64.7% for BCE (5.90% in late apoptotic stage), and ~21.6% of BCE-Eth (~71.8% in late apoptosis stage). In conclusion, our findings show that this new nanoparticle not only improves the enclosure of plant metabolites and chemotherapeutic agents but also increases the effectiveness of metabolites by increasing their controlled release and so on reduces the side effects of chemotherapy drugs.

How to cite this article
Nasri Sh., Rahaie M., Ebrahimi-Hoseinzadeh B., Hatamian-Zarmi A., Sahraeian R. A new ethosomal nanoparticle for controlled release of black cumin compounds against cancer cells. Nanomed Res J, 2021; 6(2): 158-169. DOI: 10.22034/nmrj.2021.02.007

INTRODUCTION

Breast cancer is the commonest cancer among women. Surgery, radiation therapy, and chemotherapy are common and high-risk ways to treat cancer. These methods have a detrimental effect on healthy cells and harm the patient [1]. Doxorubicin (DOX) is a type of anthracycline compounds and one of the most commonly used chemotherapy drugs used to treat malignant breast cancer. Unfortunately, despite its good properties, this drug has serious clinical side effects and severe toxic effects on healthy tissues [3]. These days, herbal ingredients are widely used as medicines for human diseases. People believe that plant materials have no side effects. However, these products have some major problems, including low accessibility for cells in the body [4]. Black cumin belongs to the Ranunculaceae family and is one of the traditional medicinal plants that have many properties such as antioxidants, anti-inflammatory, and antimicrobial. Black cumin seeds contain 22% protein in the range of 40-200 kDa and 38-40% fat, including phospholipids, lipids, and neutral glycolipids, as well as 32% carbohydrates. Black

* Corresponding Authors Email: *mrahaie@ut.ac.ir*
bahman.ebrahimi@ut.ac.ir

cumin hydroalcoholic extract has been shown to have cell toxicity activity and has been used to treat cancers as an oral administration [6, 7]. Research in mice against YAC tumors has shown that aqueous extract increases the activity of natural lethal cells by 62.3% [8]. Recently, the biological anti-tumor activity of Thymoquinone (TQ) has been proven as one of the main components of black cumin [4].

Recent research suggests that TQ, as a molecule with promising antineoplastic properties, has had effective effects on a wide range of fluid and solid tumors *in vitro* and *in vivo* models [9]. Targeting peroxisome proliferator-activated receptors (PPAR) and nuclear factor (NF)-kB associated with anticancer activity against breast cancer cell lines by TQ [10, 11]. It has been also found that TQ could inhibit the growth of colorectal cancer and cause apoptosis and control of the cell cycle of colon cancer cell line and animal models [9]. It has been shown to reduce the toxicity of TQ due to its pleiotropic properties. This toxicity is similar to that of chemotherapeutic agents such as cardiotoxicity of doxorubicin, cisplatin nephropathy, and acetaminophen hepatotoxicity. Despite its anti-cancer TQ, hydrophobicity, solubility, poor bioavailability, sensitivity to light and pH, and its binding to plasma proteins, they are the main limitations for the clinical use of this compound that prevents it from reaching the tumor site. [12, 13].

Today, nanotechnology has provided a list of useful tools for targeted drug delivery that can be achieved using nanomaterials with some modifications [14, 15]. Nanoencapsulation can improve targeted delivery capacity, greater bioavailability, and BCE protection. For example, in one project, alginate-BSO (black seed oil) beads were designed as a controlled secretion system and synthesized to control drug delivery in the gastrointestinal tract (GIT) using Electrospray technology [16]. For its active agent, TQ, several formulations of nanoparticles against prostate cancer, colorectal cancer, leukemia, multiple myeloma [17], cervical cancer, and breast cancer have been introduced [18, 19]. In this context, carriers are often used concerning cancer treatment programs, the most important of which are nanoparticles of liposomes, polymers, niosomal, solid lipids (SLN), and nanostructured lipid carriers (NLCs) [12].

Ethosomes are soft vesicles similar to liposomes which in addition to phospholipids and water, ethanol is one of their compounds. Ethosomes have been introduced to the world of science as a new vehicle for transdermal drug transmission to increase drug penetration through the skin [20, 21]. They have demonstrated a wide range of flexibility and variability, as well as high enclosure efficiency. Besides, they can efficiently provide the permeation and prescription of drugs in the skin [22]. In Ethosome, the ethanol can improve the close-fitting array of lipids in the stratum corneum and enrich their fluidity. A high concentration of ethanol enhances fluidity and membrane flexibility, as well [23, 24].

In the present study, BCE and DOX-loaded ethosomes have been synthesized and introduced to deliver transdermal drugs, with the aim of increasing BCE bioavailability as a complex of anticancer compounds. For this purpose, in addition to the complete characterization of the synthesized nanoparticles and the released dose of these compounds, experiments were performed to determine the toxicity of the cell *in vitro* and to determine the degree of skin *ex vivo* permeability with mouse skin.

EXPERIMENTAL

Materials

Cholestrol (≥99%), Phospholipon 90 (95%), DMEM (as Culture media) were purchased from Sigma-Aldrich (USA). FCS, 1% L-glutamine and penstrep were bought from Gibco (UK). Absolute Ethanol and PBS buffer were purchased from Merck (Germany) and Takara Bio Inc. (Otsu, Shiga, Japan), respectively. Doxorubicin (HCL) was obtained from Huafeng United Technology Co., Ltd. (Beijing, China). Thymoquinone (purity more than 98%) was purchased from Santa Cruz Biotechnology (USA). MCF-7 cell line was provided by the Pasture Institute of Iran. All the other materials applied in this study were analytical and pharmaceutical grade.

Extraction of Black cumin

Black cumin seeds were purchased from a local market for medicinal plants in Tehran. They were powdered by a mill. Then 50 g of this powder was mixed with 200cc of 70% ethanol and placed on the shaker for 72hours. The resulting mixture was filtered using Watman's No. 2 filter paper. This filtered mixture was concentrated using a rotary (Buchi, Germany) to completely remove ethanol. After solvent evaporation, the extract was dried by

a freeze dryer (FDB-5503, Korea). To qualify and quantify of TQ content in the extract, it used an HPLC instrument (models of 5700 solvent delivery (ESA, Bedford, MA, USA) and 7125 sample injector (Rheodyne, Cotati, CA, USA) with a 480 lambda variable wavelength UV detector (Waters, Milford, MA). A model 3392A reporting integrator (Hewlett–Packard, Avondale, PA, USA) was applied for the output signals gathering. Extractions were done using C18 PrepSep solid-phase extraction column (Fisher Scientific, Pittsburgh, PA, USA) [1].

Nanocarrier Preparation

Ethosomes were prepared using the method mentioned in Reference 26 with a slight modification [25]. The RSM statistical method was used to optimize the three main components (cholesterol, phospholipids and ethanol) of the ethosomal. BCE and DOX were added to the final concentration of 0.02 (w/v). The lipid film was hydrated with 40ml of ddH_2O at 100 rpm for 30 min at 37°C.

Characterization of Ethosomal forms

Size and Charge of Vesicles

To measure the size and distribution of vesicles, it was used Dynamic Light Scattering (DLS) technique. A little bit of ethosomes solution was diluted by 0.01 L of the hydroethanolic solution and then, it was done measurement at 25±0.5°C with 173° scattering angle (Brookhaven Instruments Corp, USA).

FT-IR Spectroscopy

In this experiment, it was used Thymoquinone as one of the BCE compounds. The FTIR spectra of samples (including TQ, BCE, DOX compounds separately, ethosomal, and optimized formulations of their) were used for the infrared analysis of them using KBr pellet technique (Shimadzu 8400S).

Differential scanning calorimetry (DSC) assay

DSC investigation was conducted to determine the physical condition of the compounds trapped inside the ethosomal vesicles. 40 µl of samples were put in an alumina pan and blank alumina was used as the reference. Fixed nitrogen gas flow was used as the inert environment. From -15 to 300°C was chosen for thermal scanning. Besides, two different temperatures of 10 and 2oC per minute were used for Ethosomal BCE, DOX, and Thymoquinone based on reference [27].

Entrapment Efficiency Analysis

In the following evaluation UV-visible spectrophotometry, The BCE and DOX entrapment efficiency (EE) of the Ethosomes passed by the Amicon filter was calculated upon the following formula:

$$EE=(Ct-Cf)/Ct\times100 \quad (1)$$

In this formula, Ct is the total amount of drug in the Ethosome and Cf is the drug diffused into solution [34].

Release profiling

The amount of the released drug was obtained according to Mohammed et al. (2014). It was carried out the release profiling in 30 ml of PBS buffer (pH 7.4) with a dialysis bag (Mw cut-off 12 kDa; Sigma) at 37°C under mild agitation (100 rpm). At fixed time intervals (48h), 20 ml of the release medium for each sample, were collected and replaced by a fresh buffer.

Stability Test

The stability of vesicles was assessed by maintenance at 4°C ± 0.5◦C. Vesicle size, zeta potential, and entrapment efficiency were evaluated after 90 days.

Ex Vivo drug permeation

A Franz diffusion cell was applied for *ex vivo* compound permeation test. The volume and area of the permeation receptor were 5 ml and 1.50 cm2, respectively. Rat abdominal skin used as a permeation barrier. The chamber was filled with a PBS buffer (pH=7.4) and it was kept at a temperature 37±1°C and 100 rpm. It was put over the Franz cell in a manner that the stratum corneum faced the donor compartment while the dermis layer was put the receptor Container. It was carefully checked the skin to ensure for any damage. 3ml was withdrawn from 0 to 48h from the sample port of the Franz cell. The receptor was immediately filled with an equal volume of fresh medium.

Bioassays

Cytotoxicity assay

Experimental samples (different concentrations of ethosomal and non-ethosomal BCE and DOX) at different volume ratios were separately added to the serum-free medium. Then, Cell viability was evaluated using the MTT assay. First, MCF-7 cells

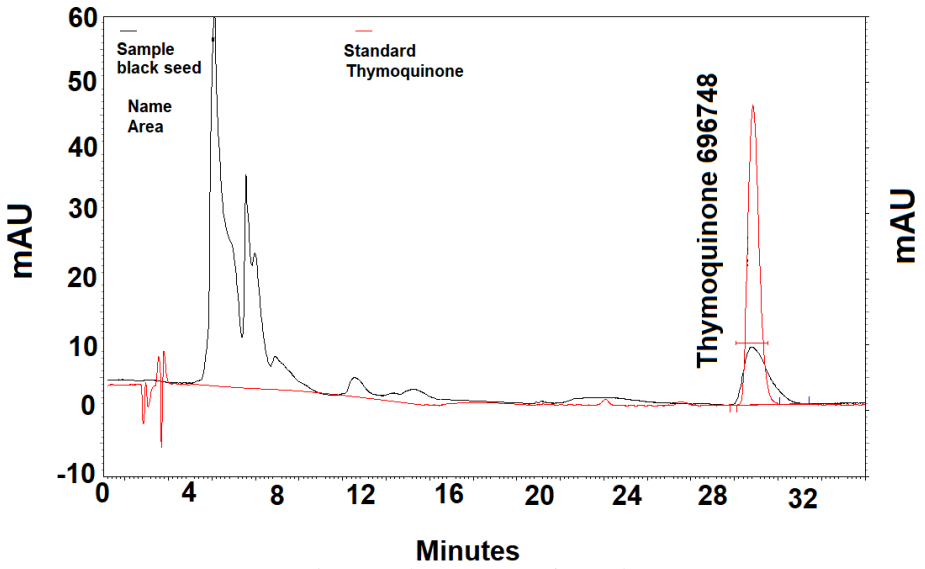

Fig.1. The HPLC chromatograms of TQ and BCE.

were grown in DMEM media containing 10% FBS, 100 U/ml penicillin, and 100 µg/ml streptomycin within a humidified incubator containing 5% CO_2 at 37°C. In follow, the cells were put in 96-well plates at a density of 5×10^3 cells per well in complete culture media and kept overnight for attachment. The free and ethosomal BCE and DOX at the next day were added into the wells and were incubated for 24, 48, and 72h. Following, to remove the residues, the cells were rinsed with PBS, and MTT was added to assay the cell viability. It was defined as relative to untreated control cells by the below equation:

$$\text{Cell viability}(\%) = (AC) \times 100 \quad (2)$$

A and C are the absorbance of the sample and control, respectively.

Apoptosis assessment

MCF-7 cell lines were grown in a 6-well plate (5 x 10^5 cells /well) and kept in a 5% of CO_2 at 37°C for 24h and then were treated with IC50 concentrations of ethosomal and non-ethosomal BCE and DOX for 48h. In follow, first, the cells were trypsinized and then were collected by centrifugation at 200 rpm. Then, they were resuspended with a binding buffer containing Annexin V-FITC and propidium iodide. After standing for 15 min at room temperature (in darkness), the cells were assessed by Flow Cytometer (BD Biosciences, USA) and FlowJo7.6 software.

RESULTS AND DISCUSSION

The HPLC Chromatography assay of hydroalcoholic extract

The chromatogram of the extract showed fine sharp peaks without any interference. The run time for TQ analysis was less than 30 min. A retention time of 29 min for TQ and 15 min for the calibration standard (TQ) were eluted (Fig.1).

The Characterization of Ethosomes

Size, Charge and Shape of Ethosomes

Ethosomes containing BCE and DOX were examined for various indicators (Table 1) including vesicle size, polydispersity index (PDI), trapping performance, and zeta potential. The results confirmed that the optimized components (including 5% soy lecithin, 45% ethanol, and 1.5% cholesterol) had the smallest vesicle size with a diameter of 20 nm and maximum entrapment efficiency of 98 ± 1%. All formulations had a Zeta potential of -42 ± 1 to -61 ± 2 mV. Ethanol and lecithin concentrations are important roles in the sustainability of ethosomes. Ethanol has a net negative charge that retains the zeta potential of the vesicles, while lecithin maintains the morphology and strength of the ethosome. The PDI was 0.12 ± 0. 011 and 0.14± 0.012. The optimized formula had a £-potential of -61±2 and a PDI of 0.14± 0.012. This formula represents the moderate distribution of vesicles among all formulas that leads to maximum stability [26].

Table 1. The Results of preliminary characterization of vesicular structure forms (n= 3).

Formulation code	Size	PDI	EE%	Zeta potential (mV)	*ex-vivo* permeation µg/ml.cm^2.hour
BCE	18.2	0.14	98 ± 1	-63	229
DOX	18.9	0.12	97 ± 1	-43	1.96

Table 2: The stability of BCE and DOX-loaded Ethosomal vesicles (T=4◦C).

Formulation	Duration of storage (Day)	PDI	EE%	Zeta potential (mV)	Size
BCE	0	0.14± 0.02	98 ± 1	-63	18.2
	90	0.21± 0.04	88± 1	-57	21± 1

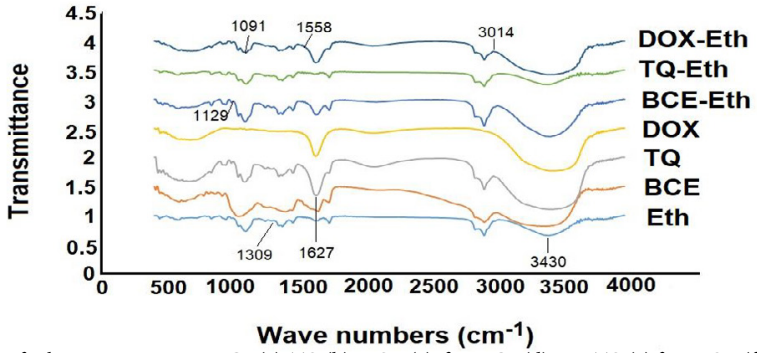

Fig.2. the IR spectrum of Ethosome containing BCE (a), TQ (b), DOX (c), free BCE (d) Free TQ (e) free DOX (f) and blank Ethosome (g).

The physical stability of the ethosomes was tested for 90 days by evaluating various parameters such as size, PDI, entrapment efficiency (EE), and zeta potential (Table 2). On day 90, significant changes (P≤0.005) were observed in the recorded parameters for ethosomes. The PDI was also less than 0.3, indicating that the particle size distribution remained stable. The zeta potential in all formulas showed stable behavior during the test. There is the possibility of vesicles fusion and then, increase of the particle size over time [26].

FTIR Spectroscopy

Fig. 2 depicts the FTIR spectra of pure BCE, TQ, and DOX and their ethosomal forms. As shown in this figure, it can be seen that the specific peaks at 3000-3500 cm-1 related to the stretching of CH, 1627cm^{-1} to the C = C stretching in the aromatic ring, the 1558 and 1524 cm ascribed to C=C in the aromatic ring, the 1309 and 1178 cm^{-1} peaks about C-N stretching and 1033 cm^{-1} which can correspond to the C=O stretching [2]. In the case of BCE, after the reaction with Ethosome, peaks were observed at 3500 cm^{-1} and 2663.91 cm^{-1}, which were related to -NH band (II) stretching or CO stretching vibrations, indicating that they may be directly involved in the ethosomic synthesis process [28].

Moreover, the peak shift from 1619 cm^{-1} to 1627 cm^{-1} illustrated that the possible C=C stretching vibration of aromatic or the C–O stretching in carboxyl or C–N bending in the amide group of vesicles. These bands display stretching vibrational bands related to some compounds like flavonoids and terpenoids [3]. There are strong vibrations at 3014 cm^{-1} in Ethosome, which corresponds to C=C-H asymmetric stretch due to the presence of ethanol. With regards to the presence of ethanol in the BCE, its graph is similar to the ethosomal graph.

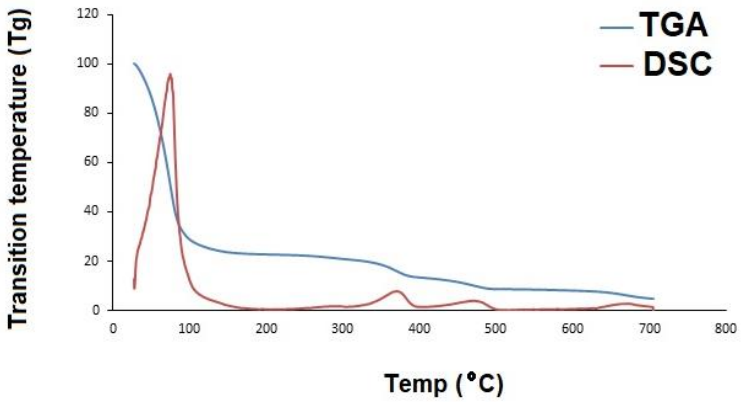

Fig.3. Differential scanning calorimetry (DSC) analysis; blank Ethosome (a) and drug-loaded Ethosome (b).

*DSC and **Entrapment Efficiency Analysis***

The DSC assay was conducted to find the drug crystallinity in selected formulations. As shown in Fig.3, a degradation peak (red graph) at 77∘C is related to the alcohol (ethanol) in the Ethosome structure and the sample weight reached 91%. Phospholipid and cholesterol degradation peaks were at 363 and 470∘C, respectively.

In the figure, TGA-DSC ethosomal BCE graph, the amount of material degraded at 73∘C was 55% and only 45% of the sample remained, which decreased this amount compared to the ethosomal sample without cargo. Therefore, the peak of the active agent is present in the extract at 77∘C.

The work showed that the melting point of BCE-Eth (56.73°C) was less than compared with raw materials (phospholipid, cholesterol, and ethanol at 363, 470, and 77∘C, respectively), but it was more than TQ (47.35∘C), which demonstrated that TQ has been dissolved in the lipid matrix and encapsulated in the lipid nanocarriers. The TQ is dissolved in the melted lipid phase during synthesis. The melting phenomenon of TQ was not detected yet. After cooling to room temperature, the lack of transition in the thermodynamic curve may be related to the TQ molecular dispersion. Reduction of the melting point of BCE-Eth (56.73∘C) and blank of Eth (57.18∘C), which was less compared with bulk material, i.e. ethanol (77∘C), is considered as "melting point depression". This event illustrated that phospholipid, cholesterol, and ethanol are being transformed into nanoparticulate forms. Ethanol in ethosomes structure makes it more fluidic, and then, the transition was seen at -14.52 ± 0.55°C (Fig.3) which was similar to the results of the previously published report by Toutiou et al. (2000). The depression of melting point is correlated to the characterization of nanoparticles (small diameter and high specific surface area). The addition of oil into the matrix changed an additional shift of the melting point to a lower temperature in both BCE-Eth and blank Eth. A reduction in melting enthalpy for Eth and BCE-Eth compared with ethanol and TQ was obtained due to its less-ordered arrangement of nanoscale particles. Hence, less amount of energy was needed to overcome the lattice force in the nanoparticles compared to ethanol. Also, incorporation of BCE inside the lipid matrix leads to a further increase in the number of defects in the lipid crystal lattice, and then it causes to slightly less melting point of BCE-Eth (56.73∘C) compared to empty Eth (57.18∘C). The defect in the crystalline lattice in BCE-Eth was proved by the high drug encapsulation efficiency and drug loading capacity (Fig.3).

In vitro release profiling and stability analysis

The measurement of entrapped compounds molecules diffusion amount was examined by their release from vesicles to the surrounding aqueous medium through dialysis bag into the medium. All the ethosomal forms represented similar release profiles as initial burst release of compounds from Ethosome followed by a constant release.

In the case of BCE, most of it was released within 2–4h, whereas, significantly ($p<0.05$), less amount of BCE released from its ethosomal form, indicated that the diffusion of it from ethosomal bilayers was the rate-limiting step in permeation through dialysis bag (Fig.4a). At first, the permeation rate due to the surface absorbed compound release [4] was higher up to 8h, which was followed by a

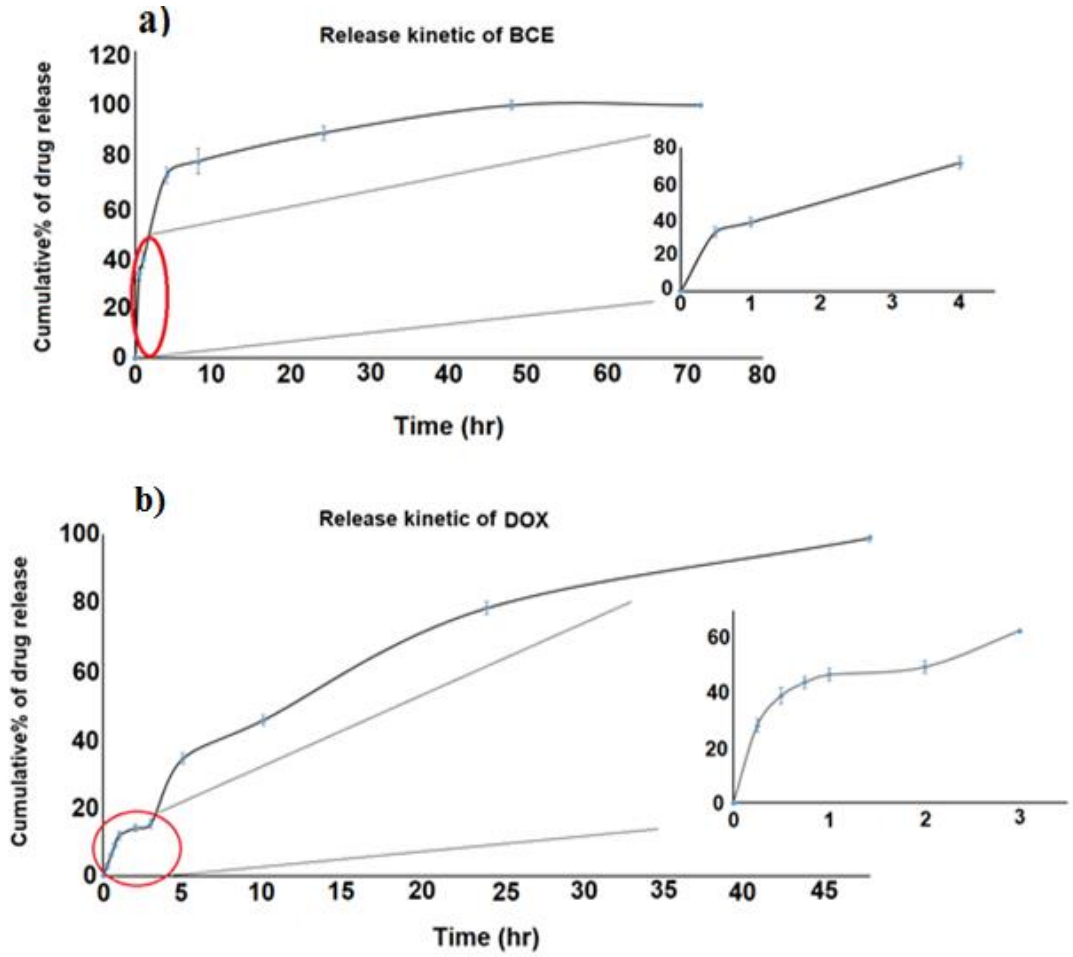

Fig.4. the profiles release of Ethosome containing BCE (a) and DOX (b). Inlet Figs are release profiles from 0-5h.

nearly zero-order release up to 24h. About 40–50% of the cargo was released in the initial phase from Ethosomes. The relatively rapid release rate may be upon the high encapsulation performance of the Ethosomes.

The *in vitro* release profiles of DOX-Eth (Fig.4b) depicted that 45.84% of the drug was released within 10h followed by more perdurable release from the nanovesicles until 24h (78.48%). Approximately, 99% of DOX was released from vesicles within 48h. The compound in Ethosomes diffused out through the surface layer. Based on the result in Fig.4b, it can be found that the release from this form depends upon the compound concentration.

Ex vivo drug permeation

Ex vivo permeation assay was conducted on rat dorsal skin using a modified diffusion cell (Fig.5). Data for the flux of BCE, TQ, and DOX across skin were obtained 229, 9.6, and 1.96 (µg/(ml.cm2.h), respectively. According to the phenomenon of mass transfer, as the initial concentration of BCE was high, the result of the driving force was higher and the flux rate was more than TQ and DOX. El Sayed et al. showed a transdermal deposition of ethosomal form of ketotifen which was significantly higher (up to 6 times) than other used delivery systems [5]. There is a list of studies that show ethosomal delivery of anti-inflammatory agents as a promising method to boost percutaneous absorption [6]. In our work, the Ethosomes were significantly improved the percutaneous permeation of BCE, TQ, and DOX through the skin ($p<0.05$). The amount of three compounds, which permeated (after 24 h), where over 40% with the use of the Ethosomes (Fig.5). Similar to our results have been found for ethosomal Linoleic acid

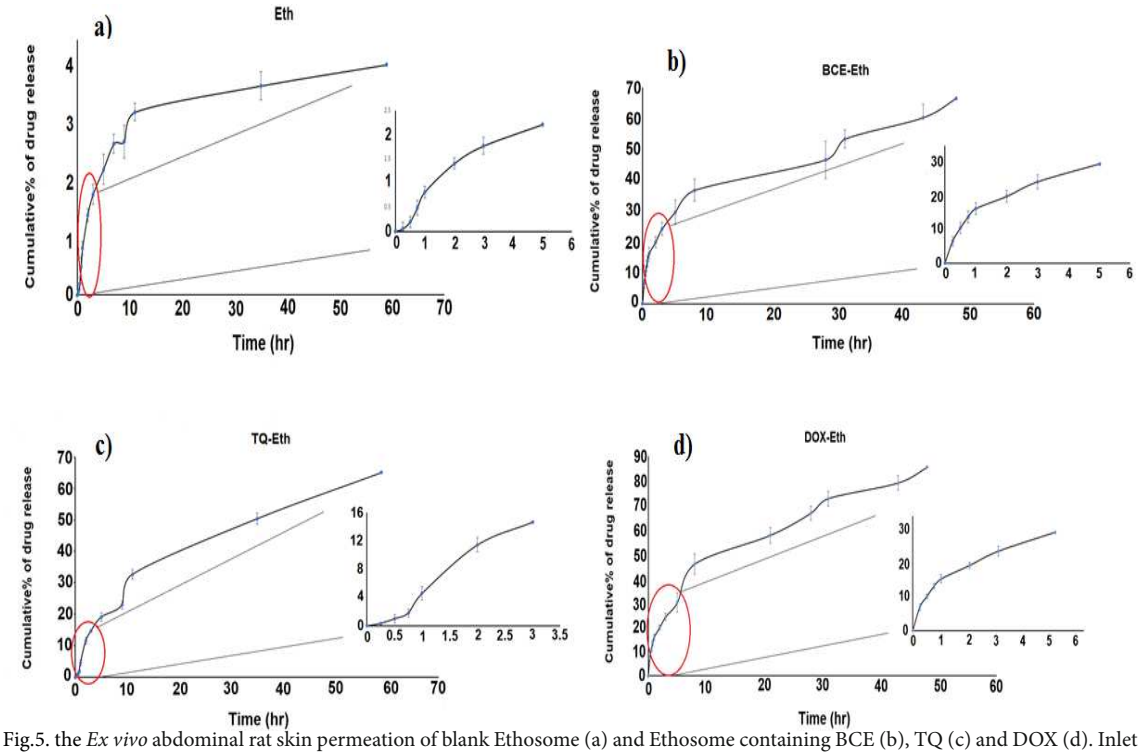

Fig.5. the *Ex vivo* abdominal rat skin permeation of blank Ethosome (a) and Ethosome containing BCE (b), TQ (c) and DOX (d). Inlet Figs are release profiles from 0-5h.

permission through the skin [7].

Specifically, a fast release of TQ and BCE was illustrated during 3h, it may be because of initial release from the outer surface bilayer. In the case of blank Ethosome, after 10h, a slow continuous release with a zero-order kinetic profile, displaying the behavior of a delivery system, was shown (Fig.5a). These effects show that a higher content of ethanol in ethosomes may enhance the molecular dynamics of cargo encapsulated in the vesicles [8] and hence, provoking the flip-flop and mobilization of unsaturated fatty acids through the bilayer, which can explain the more rapid release of drug in these vesicles.

Cytotoxicity assay

The proliferation of MCF-7 cells was significantly ($P<0.05$) inhibited by BCE, DOX, and ethosomal forms in a concentration-dependent manner in 24, 48, and 72h. It was shown that these treatments have different cytotoxicity effects on the MCF-7 cell line (Fig.6).

The IC50 assay of BCE, DOX, and their ethosomal forms on MCF-7 cell lines was conducted (Fig. 7). IC50 was assessed by Probit analysis using the Pharm Pharmacologic Calculation System (PCS) statistical package (Springer- Verlag, USA). As shown in Fig.6, the differences in IC50 values between free drug and ethosomal forms there were significantly ($P<0.05$).

In the case of BCE, IC50 value, for none and ethosomal form of BCE was 200 and 96 (µg/ml), respectively (Fig.6a). This can be due to BCE sustained release from Ethosome into the culture medium compared with free BCE.

As shown in Fig.6b, the anticancer effect of DOX-Eth was more than DOX. The results illustrated that the anti-proliferative activity of DOX-Eth was stronger than free DOX on MCF-7 ($P < 0.05$). The ethosomal DOX showed higher cytotoxicity than free DOX. This phenomenon can be due to the DOX-Eth increases the intracellular concentrations of DOX. The enhanced cellular uptake led to a predictable higher anti-proliferation effect [9]. Our results provide additional proof that the ethosomal form has more anti-cancer activity than free compounds.

Apoptosis assessment

MCF-7 cell lines were examined with an

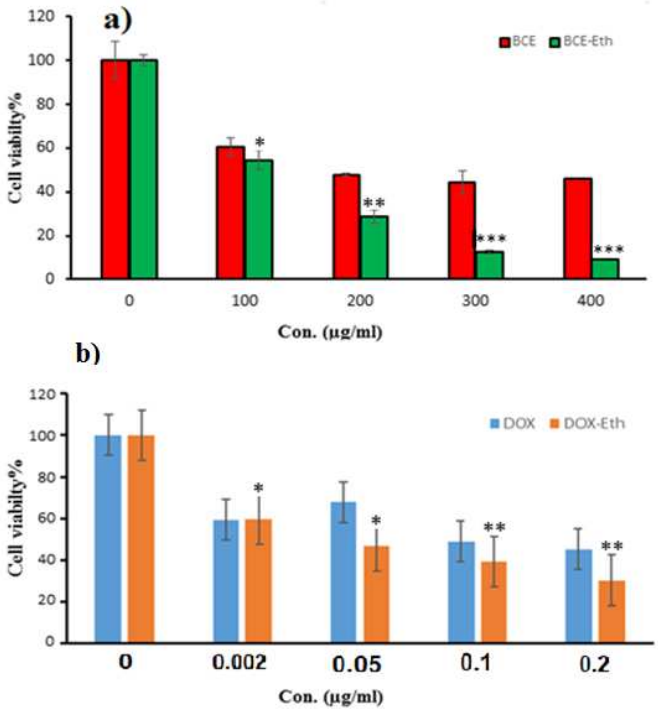

Fig.6. the MTT assay on MCF-7 cell line (in three replicates): (a) free BCE and BCE-Eth, (b) free DOX and DOX-Eth. Columns: mean (n = 3); bars: S.E. *P < 0.05; **P < 0.01, ***P < 0.001 vs. untreated cells.

Annexin V-FITC/PI staining assay. As shown in Fig.7a, the untreated cells in the control sample were mainly in good physical shape (~94.98% live cells (Q4)) with ~1.10%, ~3.02%, and ~0.91% of cells in early apoptotic (Q3), late apoptotic (Q2) and necrotic states (Q1). But, whenever the cells were treated with DOX and DOX-Eth (Fig.7b), the percent of live cells apoptotic cells decreased (~94.98% of control cells to ~65.2% in DOX, and ~31.6% of DOX-Eth treated groups) and increased, respectively. ~7.59 % and ~24.0% of free DOX treated cells were in the early and late apoptotic stages respectively. These percentages for the DOX-Eth treated cells were ~27.8% versus ~26.6% in early and late apoptosis stages respectively.

The results indicated a higher percentage of cells in the early and late apoptotic stage in the case of DOX-Eth versus pure DOX. Similar results have been obtained in the work where Doxorubicin was encapsulated in different nanostructures [10]. The greater percentage of apoptotic DOX-Eth treated cells ($p<0.05$) can be described by the increased cellular uptake and accumulation of DOX in cancer cell from the DOX contained vesicles (Fig.7b).

In the case of BCE and BCE-Eth (Fig.7c), the percent of live cells reduced from ~94.98% to ~64.7%, and ~21.6% about control cells, BCE and BCE-Eth treated cells, respectively. The free BCE treated cells exhibited ~26.2 % and ~5.90% in the early and late apoptotic stages respectively. Whereas those treated with BCE-Eth showed ~5.87% and ~71.8% in early and late apoptosis stages, respectively.

In another research, Malleswara Rao Peram et al. (2018) showed that there is a significant difference in apoptotic parameters for free curcumin and ethosomal curcumin-treated A375 cells. It clarified that ethosomes could penetrate inside the cell through the cell membrane [39]. It has been shown the human hypertrophic scar fibroblasts cells treated with 5-Aminolevulinic acid (ALA) loaded ethosomal vesicles can cause to penetrate ALA into the cells and provide higher cell apoptosis or necrosis than an ALA hydroalcoholic solution (HA) [11]. Fig.7 shows that the treated cells with empty Ethosomes had good physical shape (~85.8% live cells (Q4)) with only ~9.80%, ~0.75 % and ~3.65% of the cells were respectively in early apoptotic (Q3), late apoptotic (Q2) and necrotic states (Q1). This result suggests that ethosomal nanocarriers alone, have low toxicity to cells, and instead they have high biocompatibility.

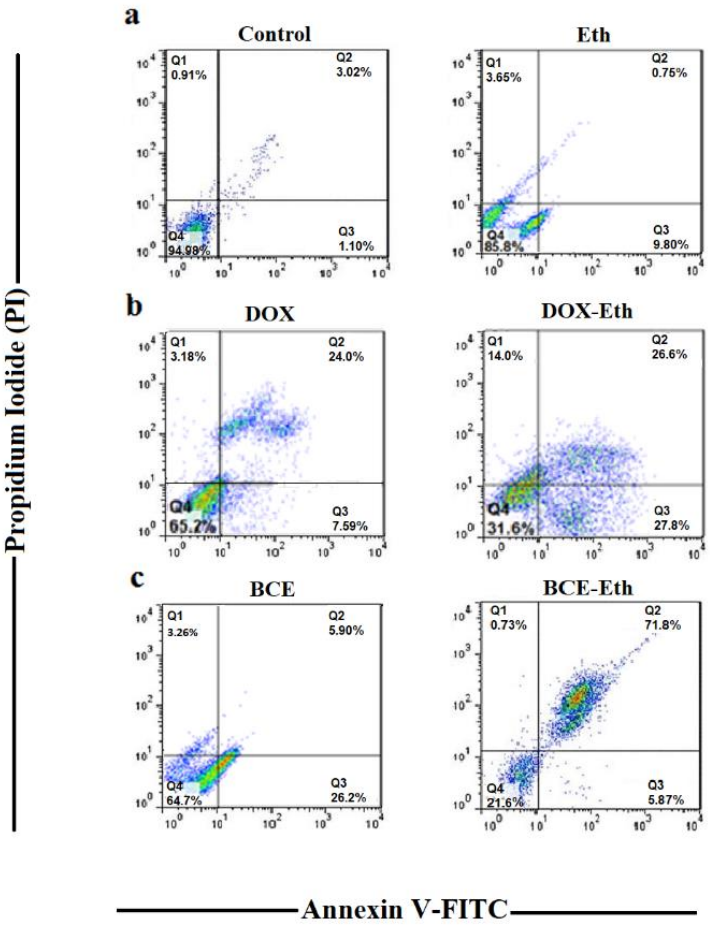

Fig.7. the flow cytometer analysis of the cellular apoptosis and oncosis after 48h of incubation (a) Control (b) free DOX and DOX-Eth, (c) free BCE and BCE-Eth, respectively MCF-7 cell lines. Q1 (necrotic states), Q2 (late apoptotic), Q3 (early apoptotic) and Q4 (live cells).

CONCLUSIONS

In this work, we synthesized and developed ethosomal BCE and DOX that can solved the low bioavailability problem of the compounds. Based on our results, the prepared forms illustrated better permeation effects in *in vitro* and *ex vivo* studies. The complete characterization was performed to show the fate of vesicles contained the compounds. FESEM, DLS, and Zeta potential studies were used to characterize the ethosomal forms for their size, shape, and bilayer formation. *Ex vivo* assay illustrated the ethosomal forms of the compounds can deliver and keep the suitable content of them which is higher versus the other transdermal release systems. MTT assay showed that IC50 values for ethosomal forms were less than the free compounds, which suggests that ethosomal forms have greater anti-cancer activity than their free state. The flow cytometry results showed enhanced apoptosis in MCF-7 cell line treated with ethosomal forms compared with free compounds. In conclusion, the findings of the research propose the ethosomal carriers can be used for bioavailability reinforcement of black cumin extract and some like natural and chemotherapeutic agents (such as DOX) on cancerous cells and provide a more efficient nanocarrier for especially transdermal release system to obtain more efficient treatment of cancerous patients.

ACKNOWLEDGMENT

We would like to thank the University of Tehran, the University of Tehran Science and Technology Park, and the NBIC center for providing financial and instrumental supports in this work.

FUNDING

This work was supported financially and instrumentally by the University of Tehran, the University of Tehran Science and Technology Park,

and the NBIC center.

CONFLICTS OF INTEREST

The authors declare that there are no conflicts of interest.

REFERENCES

1. Wang Y, Zhao R, Wang S, Liu Z, Tang R. In vivo dual-targeted chemotherapy of drug resistant cancer by rationally designed nanocarrier. Biomaterials. 2016;75:71-81.
2. Kim TH, Shin YJ, Won AJ, Lee BM, Choi WS, Jung JH, et al. Resveratrol enhances chemosensitivity of doxorubicin in multidrug-resistant human breast cancer cells via increased cellular influx of doxorubicin. Biochimica et Biophysica Acta (BBA) - General Subjects. 2014;1840(1):615-25.
3. Ambrož M, Boušová I, Skarka A, Hanušová V, Králová V, Matoušková P, et al. The Influence of Sesquiterpenes from Myrica rubra on the Antiproliferative and Pro-Oxidative Effects of Doxorubicin and Its Accumulation in Cancer Cells. Molecules. 2015;20(8):15343-58.
4. Darakhshan S, Bidmeshki Pour A, Hosseinzadeh Colagar A, Sisakhtnezhad S. Thymoquinone and its therapeutic potentials. Pharmacological Research. 2015;95-96:138-58.
5. Cui J-l, Guo S-x, Xiao P-g. Antitumor and antimicrobial activities of endophytic fungi from medicinal parts of Aquilaria sinensis. Journal of Zhejiang University SCIENCE B. 2011;12(5):385-92.

[6] M. Salomi, K. Panikkar, M. Kesavan, K. Donata Sr, K. Rajagopalan, Anti-cancer activity of nigella sativa, Ancient science of life 8(3-4) (1989) 262.

[7] R. Medenica, J. Janssens, A. Tarasenko, G. Lazovic, W. Corbitt, D. Powell, D. Jocic, V. Mujovic, Anti-angiogenic activity of Nigella sativa plant extract in cancer therapy, Proc Annu Meet Am Assoc Cancer Res, 1997, p. A1377.

8. Mahmoud SS, Torchilin VP. Hormetic/Cytotoxic Effects of Nigella sativa Seed Alcoholic and Aqueous Extracts on MCF-7 Breast Cancer Cells Alone or in Combination with Doxorubicin. Cell Biochemistry and Biophysics. 2012;66(3):451-60.
9. Schneider-Stock R, Fakhoury IH, Zaki AM, El-Baba CO, Gali-Muhtasib HU. Thymoquinone: fifty years of success in the battle against cancer models. Drug Discovery Today. 2014;19(1):18-30.
10. Woo CC, Loo SY, Gee V, Yap CW, Sethi G, Kumar AP, et al. Anticancer activity of thymoquinone in breast cancer cells: Possible involvement of PPAR-γ pathway. Biochemical Pharmacology. 2011;82(5):464-75.
11. Connelly L, Barham W, Onishko HM, Sherrill T, Chodosh LA, Blackwell TS, et al. Inhibition of NF-kappa B activity in mammary epithelium increases tumor latency and decreases tumor burden. Oncogene. 2010;30(12):1402-12.
12. Ballout F, Habli Z, Rahal ON, Fatfat M, Gali-Muhtasib H. Thymoquinone-based nanotechnology for cancer therapy: promises and challenges. Drug Discovery Today. 2018;23(5):1089-98.
13. Jain RA. The manufacturing techniques of various drug loaded biodegradable poly(lactide-co-glycolide) (PLGA) devices. Biomaterials. 2000;21(23):2475-90.
14. Mirza AZ, Siddiqui FA. Nanomedicine and drug delivery: a mini review. International Nano Letters. 2014;4(1).

[15] R.S. Soumya, P.G. Hela, Nano silver based targeted drug delivery for treatment of cancer, Der Pharmacia Lettre 5(4) (2013) 189-197.

16. Azad AK, Al-Mahmood SMA, Chatterjee B, Wan Sulaiman WMA, Elsayed TM, Doolaanea AA. Encapsulation of Black Seed Oil in Alginate Beads as a pH-Sensitive Carrier for Intestine-Targeted Drug Delivery: In Vitro, In Vivo and Ex Vivo Study. Pharmaceutics. 2020;12(3):219.
17. Shah M, Choi MH, Ullah N, Kim MO, Yoon SC. Synthesis and Characterization of PHV-Block-mPEG Diblock Copolymer and Its Formation of Amphiphilic Nanoparticles for Drug Delivery. Journal of Nanoscience and Nanotechnology. 2011;11(7):5702-10.
18. Bhattacharya S, Ahir M, Patra P, Mukherjee S, Ghosh S, Mazumdar M, et al. PEGylated-thymoquinone-nanoparticle mediated retardation of breast cancer cell migration by deregulation of cytoskeletal actin polymerization through miR-34a. Biomaterials. 2015;51:91-107.
19. Shah M, Naseer MI, Choi MH, Kim MO, Yoon SC. Amphiphilic PHA–mPEG copolymeric nanocontainers for drug delivery: Preparation, characterization and in vitro evaluation. International Journal of Pharmaceutics. 2010;400(1-2):165-75.
20. Mura S, Pirot F, Manconi M, Falson F, Fadda AM. Liposomes and niosomes as potential carriers for dermal delivery of minoxidil. Journal of Drug Targeting. 2007;15(2):101-8.
21. Hussain A, Haque MW, Singh SK, Ahmed FJ. Optimized permeation enhancer for topical delivery of 5-fluorouracil-loaded elastic liposome using Design Expert: part II. Drug Delivery. 2015;23(4):1242-53.
22. Fang J-Y, Hwang T-L, Huang Y-L, Fang C-L. Enhancement of the transdermal delivery of catechins by liposomes incorporating anionic surfactants and ethanol. International Journal of Pharmaceutics. 2006;310(1-2):131-8.
23. Xie J, Ji Y, Xue W, Ma D, Hu Y. Hyaluronic acid-containing ethosomes as a potential carrier for transdermal drug delivery. Colloids and Surfaces B: Biointerfaces. 2018;172:323-9.
24. Touitou E, Godin B, Weiss C. Enhanced delivery of drugs into and across the skin by ethosomal carriers. Drug Development Research. 2000;50(3-4):406-15.
25. Mitulovic G, Smoluch M, Chervet J-P, Steinmacher I, Kungl A, Mechtler K. An improved method for tracking and reducing the void volume in nano HPLC?MS with micro trapping columns. Analytical and Bioanalytical Chemistry. 2003;376(7):946-51.

[26] R. Vijayakumar, Formulation and evaluation of diclofenac potassium ethosomes, Madurai Medical College, Madurai, 2010.

27. Mahmood S, Mandal UK, Chatterjee B. Transdermal delivery of raloxifene HCl via ethosomal system: Formulation, advanced characterizations and pharmacokinetic evaluation. International Journal of Pharmaceutics. 2018;542(1-2):36-46.
28. Abdel Messih HA, Ishak RAH, Geneidi AS, Mansour S. Nanoethosomes for transdermal delivery of tropisetron HCl: multi-factorial predictive modeling, characterization, and ex vivo skin permeation. Drug Development and Industrial Pharmacy. 2017;43(6):958-71.
29. Baharetha HM, Nassar ZD, Aisha AF, Ahamed MBK, Al-Suede FSR, Kadir MOA, et al. Proapoptotic and Antimetastatic Properties of Supercritical CO2 Extract of Nigella sativa Linn. Against Breast Cancer Cells. Journal of Medicinal Food. 2013;16(12):1121-30.

30. Jha AK, Prasad K, Kumar V, Prasad K. Biosynthesis of silver nanoparticles using Eclipta leaf. Biotechnology Progress. 2009;25(5):1476-9.
[31] M. Liu, K. Kono, J.M. Fréchet, Water-soluble dendritic unimolecular micelles: Their potential as drug delivery agents, Journal of Controlled Release 65(1-2) (2000) 121-131.
[32] M.M. Elsayed, O. Abdallah, V. Naggar, N. Khalafallah, Deformable liposomes and ethosomes as carriers for skin delivery of ketotifen, Die Pharmazie-An International Journal of Pharmaceutical Sciences 62(2) (2007) 133-137.
33. Jangdey MS, Gupta A, Saraf S, Saraf S. Development and optimization of apigenin-loaded transfersomal system for skin cancer delivery: in vitro evaluation. Artificial Cells, Nanomedicine, and Biotechnology. 2017;45(7):1452-62.
34. Celia C, Cilurzo F, Trapasso E, Cosco D, Fresta M, Paolino D. Ethosomes® and transfersomes® containing linoleic acid: physicochemical and technological features of topical drug delivery carriers for the potential treatment of melasma disorders. Biomedical Microdevices. 2011;14(1):119-30.
35. Dubey V, Mishra D, Dutta T, Nahar M, Saraf DK, Jain NK. Dermal and transdermal delivery of an anti-psoriatic agent via ethanolic liposomes. Journal of Controlled Release. 2007;123(2):148-54.
36. Odeh F, Ismail SI, Abu-Dahab R, Mahmoud IS, Al Bawab A. Thymoquinone in liposomes: a study of loading efficiency and biological activity towards breast cancer. Drug Delivery. 2012;19(8):371-7.
37. Lin W, Xie X, Yang Y, Fu X, Liu H, Yang Y, et al. Thermosensitive magnetic liposomes with doxorubicin cell-penetrating peptides conjugate for enhanced and targeted cancer therapy. Drug Delivery. 2016;23(9):3436-43.
38. Li F, Sun J, Zhu H, Wen X, Lin C, Shi D. Preparation and characterization novel polymer-coated magnetic nanoparticles as carriers for doxorubicin. Colloids and Surfaces B: Biointerfaces. 2011;88(1):58-62.
39. Peram MR, Jalalpure S, Kumbar V, Patil S, Joshi S, Bhat K, et al. Factorial design based curcumin ethosomal nanocarriers for the skin cancer delivery: in vitro evaluation. Journal of Liposome Research. 2019;29(3):291-311.
40. Zhang Z, Chen Y, Xu H, Wo Y, Zhang Z, Liu Y, et al. 5-Aminolevulinic acid loaded ethosomal vesicles with high entrapment efficiency for in vitro topical transdermal delivery and photodynamic therapy of hypertrophic scars. Nanoscale. 2016;8(46):19270-9.